ARTICLE

Infrared-Vacuum Ultraviolet Spectroscopic and Theoretical Study of Neutral Trimethylamine Dimer[†]

Bing-bing Zhang[a,b,c‡], Xiang-tao Kong[a,c‡], Shu-kang Jiang[a,c,d,e‡], Zhi Zhao[a], Hua Xie[a], Ce Hao[b], Dong-xu Dai[a], Xue-ming Yang[a], Ling Jiang[a*]

a. State Key Laboratory of Molecular Reaction Dynamics, Collaborative Innovation Center of Chemistry for Energy and Materials (iChEM), Dalian Institute of Chemical Physics, Chinese Academy of Sciences, Dalian 116023, China
b. State Key Laboratory of Fine Chemicals, Dalian University of Technology, Dalian 116024, China
c. University of Chinese Academy of Sciences, Beijing 100049, China
d. Shanghai Advanced Research Institute, Chinese Academy of Sciences, Shanghai 201210, China
e. School of Physical Science and Technology, ShanghaiTech University, Shanghai 200031, China

Infrared-vacuum ultraviolet (IR-VUV) spectra of neutral trimethylamine dimer were measured in the $2500-3800$ cm^{-1} region. Quantum chemical calculations were performed to identify the structure of the low-lying isomers and to assign the observed spectral features. The bands at 2975 and 2949 cm^{-1} were assigned to the antisymmetric C−H stretching and the band at 2823 cm^{-1} to the symmetric C−H stretching, respectively. The 2739 cm^{-1} band was due to the CH$_3$ bending overtone, which disappeared at low IR laser power of 1 mJ/mm^2. The extra band at 2773 cm^{-1} could be due to Fermi resonance behavior of the light isotopologue, these are often close in energy and can strongly mix through cubic terms in the potential function. Experimental and theoretical results indicate the likely coexistence of multiple structures. The peak widths of IR spectra of neutral trimethylamine dimer are not significantly affected by the structural transformation, allowing the stretching modes to be well resolved.

Key words: Infrared-vacuum ultraviolet, Neutral cluster, Trimethylamine, Quantum chemical calculation

I. INTRODUCTION

As organic solvents and reagents, amines are ubiquitous in biology and play an important role in enhancing particle nucleation and growth and affecting secondary organic aerosol formation [1, 2]. Atmospheric amines are emitted from various biogenic (such as ocean organisms, protein degradation, and biomass burning) and anthropogenic (such as animal husbandry, automobiles, industries, and treatment of sewage and waste) sources [3]. Global emission of amines from animal husbandry operations was estimated to be $\sim 95-198$ Gg nitrogen/year, with trimethylamine (TMA, (CH$_3$)$_3$N) being the most prevalent [4]. TMA was observed to be an important precursor formation of the critical nucleus under different ambient environments [5].

Mass spectrometry and optical spectroscopy of gas-phase clusters provide detailed energetic and structural information that is difficult to extract from bulk measurement [6−14]. Infrared photodissociation (IRPD) spectroscopy of H$^+$(TMA)$_n$H$_2$O (n=1−22) clusters has demonstrated that the proton localizes on the TMA moiety regardless of cluster size [15, 16]. IRPD spectroscopic study of H$^+$TMA(benzene)$_n$ (n=1−4) clusters indicated that the methyl groups of protonated trimethylamine are solvated by benzene [17]. Matrix-isolation IR study of TMA/H$_2$O clusters showed that the cluster is formed in the vapor phase (as opposed to being a result of diffusion of the trapped species) and is related to its large stabilization energy (enthalpy) because of strong cooperative effects in its H-bond system [18]. In the TMA/H$_2$SO$_4$/H$_2$O clusters, the complex formed between TMA and H$_2$SO$_4$ is of ionic character due to proton transfer of the H$^+$ proton from H$_2$SO$_4$ to TMA to form a new N−H bond and the replacement of the intramolecular O−H bond in H$_2$SO$_4$ by a strong intermolecular N−H$\cdots$O hydrogen bond [19]. Recent IRPD spectroscopy of (TMA)$_2$$^+$ cation suggests the coexistence of the N$\cdots$N and C$\cdots$HN structures [20].

In contrast, much less work has been done for neutral solvation clusters, due to difficulties in both size selec-

---

tion and signal detection. The preliminary IR spectrum of the neutral $(TMA)_2$ reported previously was not resolved well and the structural and dynamic information was eluded [20]. Herein, we report the use of infrared-vacuum ultraviolet (IR-VUV) spectroscopy to probe the neutral TMA dimer. IR power dependence was performed to check the saturation effect and to gain a better spectral resolution. Quantum chemical calculations were performed to identify the structure of the low-lying isomers and to assign the observed spectral features.

II. EXPERIMENTS

Experiments were performed using the Dalian IR-VUV apparatus, which consists of a pulsed supersonic cluster source and a reflectron time-of-flight (TOF) mass spectrometer. Details of the apparatus have been described previously [21], and only a brief outline is given below. The VUV light at 118 nm used in this study was generated by third harmonic generation (355 nm) of a Nd:YAG laser (Nimma-600) via Xe/Ar gas mixture at 1:10 relative concentration for 200 Torr total pressure. A beam of neutral complexes was generated from supersonic expansions of 5% TMA seeded in He using a pulsed valve (General Valve, Series 9) at 5 atm backing pressure and passed through a 4 mm diameter skimmer and an aperture with 3 mm opening. The cations were produced from the 118 nm one-photon ionization process in the center of the extraction region of a reflectron TOF mass spectrometer and the signal intensity of the particular mass channel was monitored. Here, the tunable IR light pulse was introduced at about 30 ns prior to the VUV laser pulse in a crossed manner. When the resonant vibrational transition with the IR light caused vibrational predissociation, the dissociation induced depopulation of the neutral cluster. The depopulation can be monitored as a reduction of the ion signal intensity in the cluster mass channel. An IR spectrum of the size-selected neutral species was obtained as a depletion spectrum of the monitored ion signal intensity by scanning the IR wavelength. The VUV laser was operated at 20 Hz and IR laser was operated at 10 Hz. IR spectra were recorded in the difference mode of operation.

The tunable IR laser beam was generated by a KTP/KTA optical parametric oscillator/amplifier system (OPO/OPA, LaserVision) pumped by an injection-seeded Nd:YAG laser (Continuum Surelite EX). This system is tunable from 700 cm^{-1} to 7000 cm^{-1} with a line width of 1 cm^{-1}. The wavelength of the OPO laser output was calibrated using a commercial wavelength meter (Bristol, 821 Pulse Laser Wavelength Meter). IR spectrum was determined from the relative depletion of the mass spectrometric ion signal using the following equation:

$$\sigma = \frac{-\ln[I(\nu)/I_0]}{P(\nu)} \qquad (1)$$

where $I(\nu)$ and I_0 are the depletion of the mass spectrometric ion signal and the mass spectrometric signal of parent ion, respectively, and $P(\nu)$ is the frequency-dependent laser power. The normalization with the IR laser pulse energy accounted for its variations over the tuning range.
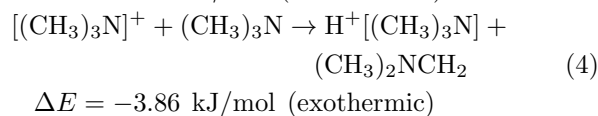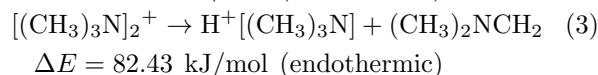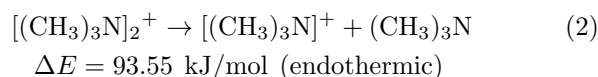
III. THEORETICAL METHOD

Quantum chemical calculations were carried out using the Gaussian 09 package [22]. Recent investigations have demonstrated that the M06-2X/6-311+G(d,p) method can well reproduce the infrared spectroscopic experiments of neutral methylamine clusters [21], which was also employed for the present calculations. Relative energies and binding energies included the zero-point-energy corrections. Harmonic and anharmonic vibrational frequencies were calculated with analytical second derivatives. A scaled factor of 0.955 was used for M062X/6-311+G(d,p) harmonic vibrational frequencies, in order to account for anharmonicities and for the method-dependent systematic errors on the calculated harmonic force constants. The resulting stick spectra were convoluted by a Gaussian line shape function with a width of 6 cm^{-1} (FWHM).

IV. RESULTS AND DISCUSSION

A. Experimental results

Typical mass spectrum of the cations produced by the 118 nm one-photon ionization of TMA clusters is shown in FIG. 1. Two series of TMA cluster cations are observed, one unprotonated $((TMA)_n^+)$ and the other protonated $(H^+(TMA)_n)$. Protonated cations are often produced when clusters of alcohol or amine are ionized. For the IR-VUV measurement, it has been addressed by previous studies, for example, in the cases of methanol [23] and ammonia [24]. With a proton affinity $\sim$949 kJ/mol [25], TMA could also easily pick up a proton.

Reactions (2) and (3) were predicted to be endothermic by 93.55 and 82.43 kJ/mol, respectively, whereas reaction (4) was estimated to be exothermic by 3.86 kJ/mol. Most of the excess energy in this VUV one-photon ionization will be taken away by the neutral fragment products.

$$[(CH_3)_3N]_2^+ \rightarrow [(CH_3)_3N]^+ + (CH_3)_3N \qquad (2)$$
$$\Delta E = 93.55 \text{ kJ/mol (endothermic)}$$
$$[(CH_3)_3N]_2^+ \rightarrow H^+[(CH_3)_3N] + (CH_3)_2NCH_2 \qquad (3)$$
$$\Delta E = 82.43 \text{ kJ/mol (endothermic)}$$
$$[(CH_3)_3N]^+ + (CH_3)_3N \rightarrow H^+[(CH_3)_3N] +$$
$$(CH_3)_2NCH_2 \qquad (4)$$
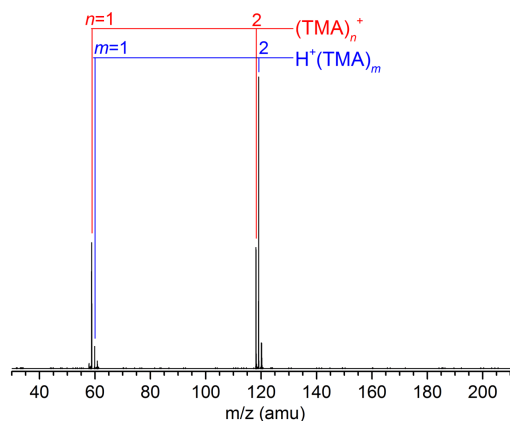$$\Delta E = -3.86 \text{ kJ/mol (exothermic)}$$

FIG. 1 Time-of-flight mass spectrum of the cations produced from the 118 nm one-photon ionization process in a pulsed supersonic expansion of 5% TMA seeded in He.

FIG. 2 IR laser power dependence for infrared spectra of neutral $(TMA)_2$. The best resolution was achieved at the experimental condition (c) with an average energy of IR laser pulse of ~ 1 mJ/mm^2 compared to the other two experimental conditions (a) 6.7/8.8 mJ/mm^2 and (b) 4.5/5.8 mJ/mm^2.

During our experiment, various conditions (type of nozzle, concentration, and stagnation pressure) were optimized so that the VUV ionization of a supersonic jet of 5% TMA/He mixture produced a mass spectrum with very small signal intensities for unprotonated and protonated trimer and larger clusters (FIG. 1). It can be seen from FIG. 1 that no obvious mass spectral signals of $(TMA)_3^+$ and $H^+(TMA)_3$ are observed, suggesting the $n \geq 3$ clusters are not readily formed under the present experimental conditions. When the tunable IR laser pulse was introduced at about 30 ns prior to the VUV pulse, the depletion spectrum obtained by monitoring the intensity of the $(TMA)_2^+$ mass channel and scanning the IR frequency in the $2500-3800$ cm^{-1} region (FIG. 2) was attributed to the vibrational predissociation of the neutral $(TMA)_2$. The experimental IR spectra comprise four groups of intense bands labeled A, B, C, D, which are well resolved rather than the previous work [20]. Experimental frequencies of $(TMA)_2$ are summarized in Table I.

IR laser power dependence was performed to check the saturation effect as shown in FIG. 2. Bands A−D were observed at the experimental conditions (FIG. 2 (a) and (b)), respectively. Band D (2739 cm^{-1}) was absent at the experimental condition (FIG. 2(c)) with low IR laser power of ~ 1 mJ/mm^2. As demonstrated before for the first overtone of the antisymmetric O−H stretching in the IRPD spectra of $[MgNO_3(H_2O)_n]^+$ ($n=1-3$) [26], the intensity of a higher order excitation is more sensitive to the IR laser power. Band D fits such a behavior very well, with its disappearance at low IR laser power, and is assigned to an overtone or combination band.

B. Comparison of experimental and theoretical results

Quantum chemical calculations simulations were performed to interpret the experimental IR spectra and
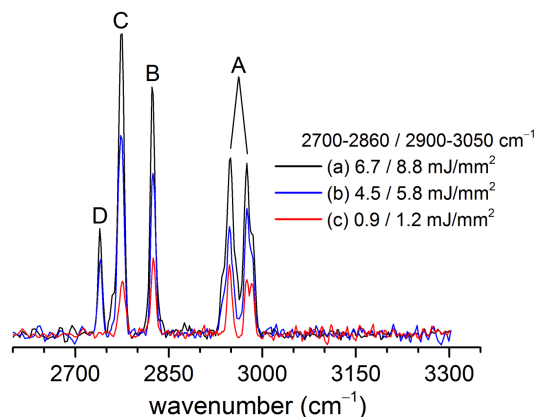
TABLE I Experimental IR-VUV band positions (cm^{-1}), M062X calculated harmonic frequencies (cm^{-1}), and band assignments for the four lowest energy isomers of neutral $(TMA)_2$ including 2-I, 2-II, 2-III, 2-IV.

Label	Expt.	2-I	2-II	2-III	2-IV	Assignment
A	2975	2985	2985	2986	2997	$\nu_{a(C-H)}$
	2949	2939	2945	2944	2952	
B	2823	2828	2827	2855	2830	$\nu_{s(C-H)}$
				2845	2815	
				2832	2803	
C	2773					Fermi resonance
D	2739	2790	2755	2803	2800	CH$_3$ bending overtone

structural dynamics of $(TMA)_2$. The structures, energetics, and simulated linear absorption spectra of the four lowest-lying isomers (2-I, 2-II, 2-III, 2-IV) are shown together with the corresponding experimental IR spectrum in FIG. 3. The lowest-energy isomer, labeled 2-I, is a C_{2h} structure in which four N$\cdots$H H-bonds are formed in-between the two TMA molecules. The 2-II isomer is a C_s structure and also consists of four N$\cdots$H H-bonds, which lies 4.74 kJ/mol higher in energy than 2-I. In the third isomer (C_3), 2-III, the TMA molecules form three N$\cdots$H H-bonds, which lies 8.27 kJ/mol above 2-I. The 2-IV isomer (+9.37 kJ/mol) is a C_s structure and consists of two N$\cdots$H H-bonds.

In the calculated IR spectrum of 2-I, the antisymmetric C−H stretchings ($\nu_{a(C-H)}$) are calculated to be 2985 and 2939 cm^{-1} (FIG. 3 and Table I), which well reproduce band A (2975 and 2949 cm^{-1}). The symmetric C−H stretching ($\nu_{s(C-H)}$) is calculated to be centered around 2828 cm^{-1}, which nicely reproduces band B (2823 cm^{-1}). The CH$_3$ bending overtone is predicted at 2790 cm^{-1} (Table I). Similarly, the 2-II iso-

mer yields calculated positions of bands A and B which are in excellent agreement with the experimental values (FIG. 3 and Table I). In the calculated IR spectrum of 2-III, band B is split into three distinct features, which are not observed experimentally. Analogous splitting of band B also appears in the calculated IR spectrum of 2-IV. Summarizing, the calculated IR spectra of 2-I and 2-II agree best with experiment, except that band C (2773 cm^{-1}) is not reproduced in the calculated harmonic vibrational spectra. The isomerization barrier from 2-II to 2-I energy difference is ∼0.1 kJ/mol, indicating that the transformation between these two isomers is facile. The coexistence of the 2-I and 2-II isomers is likely here.

The extra band C could be due to Fermi resonance behavior of the light isotopologue, these are often close in energy and can strongly mix through cubic terms in the potential function [18, 27, 28]. An intense band of Fermi-mixing type was observed at 2820 cm^{-1} in the H$^+$(TMA)H$_2$O cluster [18]. In the C−H Fermi resonances in the formate ion reported recently [27], the dominant interactions occur between the C−H stretch fundamental and both the in-plane and out-of-plane bending overtones. Multidimensional anharmonic calculations to clarify the source of band C in the IR spectrum of (TMA)$_2$ are in progress.

In summary, the peak widths of IR spectra of neutral trimethylamine dimer are not significantly affected by the structural transformation, allowing the stretching modes to be well resolved. This is similar to the dynamic nature of (CH$_3$NH$_2$)$_2$ with the involvement of fast configuration interconversion of *cis* and *trans* dimer [21]. Our current experimental setup is limited by the wavelength and peak power of the tabletop VUV laser, which could only ionize molecules with appropriate ionization potentials. This limit could be easily removed by using a VUV free electron laser (50−150 nm), such as the one under construction in Dalian Institute of Chemical Physics, which shall make it possible to measure a wide variety of neutral solvation clusters, providing fundamental details into the microsolvation of organic molecules and solvent-solvent interactions.

V. CONCLUSION

The approach of IR-VUV spectroscopy combined with quantum chemical calculation was employed to study the CH$_3$ vibrational spectral patterns of neutral trimethylamine dimer. The bands at 2975 and 2949 cm^{-1} were assigned to the antisymmetric C−H stretching and band at 2823 cm^{-1} to the symmetric C−H stretching, respectively. The 2739 cm^{-1} band was due to the CH$_3$ bending overtone, which disappeared at low IR laser power of 1 mJ/mm^2. The extra band at 2773 cm^{-1} could be due to Fermi resonance. The coexistence of multiple isomers is likely for trimethylamine dimer, which is consistent with the small pre-
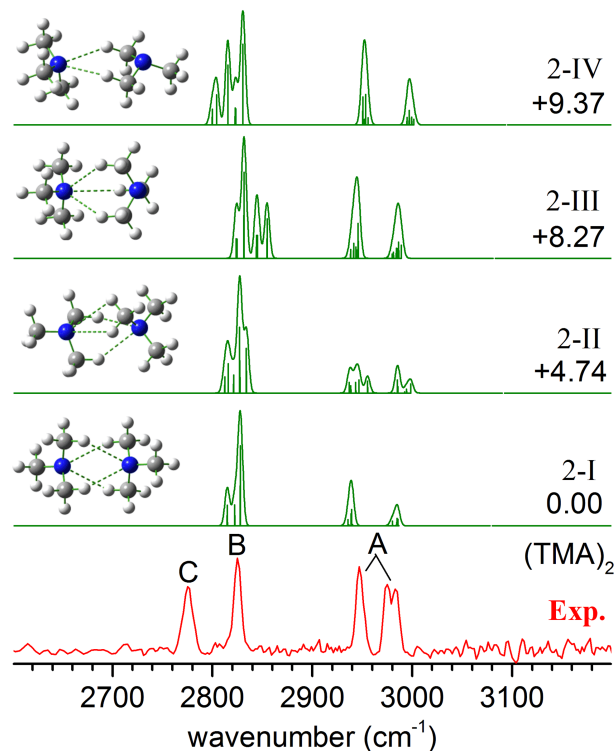

FIG. 3 Experimental IR spectrum of neutral (TMA)$_2$ (bottom row), with the simulated linear absorption spectra, structures, and relative energies (kJ/mol) of the four lowest-energy isomers of 2-I, 2-II, 2-III, 2-IV. The average energy of IR laser pulse was 1 mJ/mm^2.

dicted energy difference between the two configurations separated by low barriers. The ability to decipher such isomers where very subtle forces and energies are at play, suggests that the present method could be applied to larger complexes and clusters which are directly relevant to the fields of chemical biology and atmospheric chemistry.

VI. ACKNOWLEDGMENTS

[1] R. Zhang, A. Khalizov, L. Wang, M. Hu, and W. Xu, Chem. Rev. **112**, 1957 (2012).
[2] M. Kulmala, J. Kontkanen, H. Junninen, K. Lehtipalo, H. E. Manninen, T. Nieminen, T. Petaja, M. Sipila, S. Schobesberger, P. Rantala, A. Franchin, T. Jokinen, E. Jarvinen, M. Aijala, J. Kangasluoma, J. Hakala, P. P.

Aalto, P. Paasonen, J. Mikkila, J. Vanhanen, J. Aalto, H. Hakola, U. Makkonen, T. Ruuskanen, R. L. Mauldin, III, J. Duplissy, H. Vehkamaki, J. Back, A. Kortelainen, I. Riipinen, T. Kurten, M. V. Johnston, J. N. Smith, M. Ehn, T. F. Mentel, K. E. J. Lehtinen, A. Laaksonen, V. M. Kerminen, and D. R. Worsnop, Science **339**, 943 (2013).

[3] X. Ge, A. S. Wexler, and S. L. Clegg, Atmos. Environ. **45**, 524 (2011).

[4] G. W. Schade and P. J. Crutzen, J. Atmos. Chem. **22**, 319 (1995).

[5] P. J. Silva, M. E. Erupe, D. Price, J. Elias, Q. G. J. Malloy, Q. Li, B. Warren, and D. R. Cocker III, Enviro. Sci. Technol. **42**, 4689 (2008).

[6] T. S. Zwier, Annu. Rev. Phys. Chem. **47**, 205 (1996).

[7] J. J. Scherer, J. B. Paul, A. Okeefe, and R. J. Saykally, Chem. Rev. **97**, 25 (1997).

[8] B. Brutschy, Chem. Rev. **100**, 3891 (2000).

[9] U. Buck and F. Huisken, Chem. Rev. **100**, 3863 (2000).

[10] C. E. H. Dessent and K. Muller-Dethlefs, Chem. Rev. **100**, 3999 (2000).

[11] A. B. Wolk, C. M. Leavitt, E. Garand, and M. A. Johnson, Acc. Chem. Res. **47**, 202 (2014).

[12] N. Heine and K. R. Asmis, Int. Rev. Phys. Chem. **34**, 1 (2015).

[13] O. Dopfer and M. Fujii, Chem. Rev. **116**, 5432 (2016).

[14] X. B. Wang, J. Phys. Chem. A **121**, 1389 (2017).

[15] R. Shishido, J. L. Kuo, and A. Fujii, J. Phys. Chem. A **116**, 6740 (2012).

[16] R. Shishido, Y. C. Li, C. W. Tsai, D. Bing, A. Fujii, and J. L. Kuo, Phys. Chem. Chem. Phys. **17**, 25863 (2015).

[17] R. Shishido, Y. Kawai, and A. Fujii, J. Phys. Chem. A **118**, 7297 (2014).

[18] M. Rozenberg, A. Loewenschuss, and C. J. Nielsen, J. Phys. Chem. A **116**, 4089 (2012).

[19] M. Rozenberg, A. Loewenschuss, and C. J. Nielsen, J. Phys. Chem. A **118**, 1004 (2014).

[20] Y. Matsuda, Y. Nakayama, N. Mikami, and A. Fujii,

Phys. Chem. Chem. Phys. **16**, 9619 (2014).

[21] B. Zhang, X. Kong, S. Jiang, Z. Zhao, D. Yang, H. Xie, C. Hao, D. Dai, X. Yang, Z. F. Liu, and L. Jiang, J. Phys. Chem. A **121**, 7176 (2017).

[22] M. J. Frisch, G. W. Trucks, H. B. Schlegel, G. E. Scuseria, M. A. Robb, J. R. Cheeseman, G. Scalmani, V. Barone, B. Mennucci, G. A. Petersson, H. Nakatsuji, M. Caricato, X. Li, H. P. Hratchian, A. F. Izmaylov, J. Bloino, G. Zheng, J. L. Sonnenberg, M. Hada, M. Ehara, K. Toyota, R. Fukuda, J. Hasegawa, M. Ishida, T. Nakajima, Y. Honda, O. Kitao, H. Nakai, T. Vreven, J. A. Montgomery, J. E. Peralta, F. Ogliaro, M. Bearpark, J. J. Heyd, E. Brothers, K. N. Kudin, V. N. Staroverov, R. Kobayashi, J. Normand, K. Raghavachari, A. Rendell, J. C. Burant, S. S. Iyengar, J. Tomasi, M. Cossi, N. Rega, J. M. Millam, M. Klene, J. E. Knox, J. B. Cross, V. Bakken, C. Adamo, J. Jaramillo, R. Gomperts, R. E. Stratmann, O. Yazyev, A. J. Austin, R. Cammi, C. Pomelli, J. W. Ochterski, R. L. Martin, K. Morokuma, V. G. Zakrzewski, G. A. Voth, P. Salvador, J. J. Dannenberg, S. Dapprich, A. D. Daniels, Ö. Farkas, J. B. Foresman, J. V. Ortiz, J. Cioslowski, and D. J. Fox, *Gaussian 09, Revision A02*, Wallingford, CT: Gaussian Inc., (2009).

[23] H. L. Han, C. Camacho, H. A. Witek, and Y. P. Lee, J. Chem. Phys. **134**, 144309 (2011).

[24] Y. Matsuda, M. Mori, M. Hachiya, A. Fujii, and N. Mikami, Chem. Phys. Lett. **422**, 378 (2006).

[25] E. P. L. Hunter and S. G. Lias, J. Phys. Chem. Ref. Data **27**, 413 (1998).

[26] L. Jiang, T. Wende, R. Bergmann, G. Meijer, and K. R. Asmis, J. Am. Chem. Soc. **132**, 7398 (2010).

[27] H. K. Gerardi, A. F. DeBlase, X. Su, K. D. Jordan, A. B. McCoy, and M. A. Johnson, J. Phys. Chem. Lett. **2**, 2437 (2011).

[28] Y. Q. Yu, Y. X. Wang, K. Lin, N. Y. Hu, X. G. Zhou, and S. L. Liu, J. Phys. Chem. A **117**, 4377 (2013).